Decreased embryonic retinoic acid synthesis results in a DiGeorge syndrome phenotype in newborn mice

Julien Vermot, Karen Niederreither*, Jean-Marie Garnier, Pierre Chambon, and Pascal Dollé†

Institut de Génétique et de Biologie Moléculaire et Cellulaire, Centre National de la Recherche Scientifique/Institut National de la Santé et de la Recherche Médicale/Université Louis Pasteur/Collège de France, BP 10142, 67404 Illkirch Cedex, Communauté Urbaine de Strasbourg, France

Contributed by Pierre Chambon, December 27, 2002

Retinoic acid (RA), the active derivative of vitamin A, is involved in various developmental and homeostatic processes. To define whether certain developmental events are particularly sensitive to a decrease in embryonic RA levels, we generated mice bearing a hypomorphic allele of the RA-synthesizing enzyme *Raldh2*. The resulting mutant mice, which die perinatally, exhibit the features of the human DiGeorge syndrome (DGS) with heart outflow tract septation defects and anomalies of the aortic arch-derived head and neck arteries, laryngeal-tracheal cartilage defects, and thymus/parathyroid aplasia or hypoplasia. Analysis of *Raldh2* hypomorph embryos reveal selective defects of the posterior (third to sixth) branchial arches, including absence or hypoplasia of the corresponding aortic arches and pharyngeal pouches, and local down-regulation of RA-target genes. Thus, a decreased level of embryonic RA (through genetic and/or nutritional causes) could represent a major modifier of the expressivity of human 22q11del-associated DiGeorge/velocardiofacial syndromes and, if severe enough, could on its own lead to the clinical features of the DiGeorge syndrome.

Retinoic acid (RA), the active vitamin A (retinol) derivative, is involved in numerous vertebrate developmental processes. RA acts as a ligand for nuclear receptors (RARs), which exist as three distinct isotypes (RARα, -β, and -γ) and bind as heterodimers with retinoid X receptors to regulatory DNA sequences known as RA response elements (RAREs) (reviewed in refs. 1 and 2). All three RARs are expressed during mouse development, either in an almost ubiquitous manner (for RARα) or in more complex, tissue-specific patterns (for RARβ and -γ; ref. 3 and references therein). Gene-targeting studies have shown that these receptors may function in a redundant manner during development (ref. 4 and references therein). Whereas null mutation for any given receptor leads to viable mice, compound mutations of any receptor pair result in pleiotropic developmental defects that recapitulate the spectrum of abnormalities generated by dietary vitamin A deficiency in rodents (5).

Two enzymatic reactions convert retinol, which in mammalian embryos is supplied transplacentally from the maternal circulation, into RA. The retinaldehyde (Ral) to RA conversion can be carried out by three members of the aldehyde dehydrogenase family, the retinaldehyde dehydrogenases (RALDH) 1, 2, and 3 (also known as ALDH1A1, -A2, and -A3) (6, 7). Among these, RALDH2 is expressed from gastrulation onward, and its expression sites correlate with many of the regions that were shown to contain RA during early embryogenesis (8). Homozygous disruption of the mouse *Raldh2* gene is early [around embryonic day (E)10.5] embryonic lethal, because of defects in heart morphogenesis (9, 10). Abnormal patterning of the hindbrain and altered somitic development are also seen (9, 11).

It is yet unclear whether certain developmental events are especially sensitive to a decrease, rather than a complete lack, of RA signaling. This is, however, an important issue in the context of human embryology, because situations of decreased function (e.g., through heterozygous mutations of *RALDH2* or *RAR* genes) are likely to occur more frequently than conditions that disrupt RA signaling. To address this question, we took advantage of a murine *Raldh2* allele (*Raldh2*^{neo}) that was generated to allow conditional mutagenesis and harbors an intronic neo-selectable marker. We show that this allele behaves as a hypomorph, and that the corresponding mutant mice die perinatally. Interestingly, these mice exhibit a limited set of abnormalities that phenocopy the human DiGeorge syndrome (DGS), a relatively frequent birth disorder characterized by heart outflow tract septation defects, abnormal patterning of the aortic arch derivatives, and hypoplasia or aplasia of the thymus and parathyroid glands (12, 13).

Methods

Gene Targeting. A 15-kb *Raldh2* genomic clone was isolated from a mouse 129/sv genomic library by using a *Raldh2* cDNA probe. *Eco*RI and *Kpn*I restriction sites were generated in introns 3 and 4, respectively, by site-directed mutagenesis. These sites were used to introduce, respectively, a synthetic double-stranded oligonucleotide containing an antisense *loxP* site and a *Nsi*I restriction site, and a *loxP*-flanked *PGK-neo*-poly(A) cassette. The linearized targeting construct was electroporated into embryonic stem (ES) cells, and homologous recombination was identified in 3 of 250 G418-resistant clones by using 5′- and 3′-flanking probes (see Fig. 1*A*). *Raldh2*$^{neo/+}$ ES cells were injected in C57BL/6 blastocysts, which were reimplanted into CD1 pseudopregnant females to produce chimeric mice. Germline transmission was observed with five of the chimeric males.

Mouse Analysis. *Raldh2*$^{neo/+}$ mice were intercrossed or crossed with *Raldh2*$^{+/-}$ CD1 mice to generate *Raldh2*$^{neo/neo}$ and *Raldh2*$^{neo/-}$ mutants, respectively. Genotype was assessed by PCR analysis of tail or yolk sac genomic DNA (primer sequences and PCR conditions are available on request). Histological analysis and whole-mount immunohistochemistry were performed as described (14). Skeletal stainings were performed without removal of internal organs, thus allowing staining of the large arteries. Whole-mount *in situ* hybridization (ISH) was performed (15) by using plasmids kindly provided by G. Barsh (Stanford University, Stanford, CA: *kreisler*), D. Duboule (Geneva University, Geneva: *lacZ*), R. Krumlauf (Stowers Institute, Kansas City, MO: *Hoxb1*), and V. Papaioannou (Columbia University, New York: *Tbx1*). Ink injections were carried out in the left ventricle by using a 1-mm capillary tube, and embryos were analyzed extemporaneously. Whole-mount 5-bromo-4-chloro-3-indolyl β-D-galactoside assays were performed as described (16), with a 2.5-h incubation period at 37°C.

Abbreviations: DGS, DiGeorge syndrome; ES, embryonic stem; ISH, *in situ* hybridization; LSA, left subclavian artery; NCC, neural crest cells; PTA, persistent truncus arteriosus; RA, retinoic acid; RALDH, retinaldehyde dehydrogenase; RAR, RA receptor; RARE, RA response element; RSA, right subclavian artery; VCFS, velocardiofacial syndrome; E*n*, embryonic day *n*; P*n*, postnatal day *n*.

*Present address: Departments of Medicine and Molecular and Cellular Biology, Center for Cardiovascular Development, Baylor College of Medicine, One Baylor Plaza, Houston, TX 77030.

†To whom correspondence should be addressed. E-mail: dolle@igbmc.u-strasbg.fr.

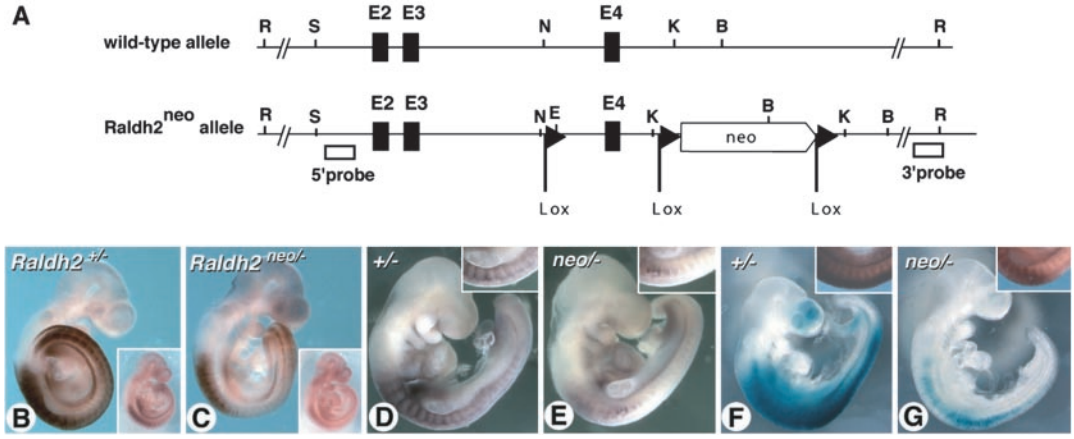

Fig. 1. Generation of a Raldh2 hypomorphic allele. (*A*) Scheme of the Raldh2 WT allele and the Raldh2^{neo} allele after homologous recombination in ES cells. B, *Bam*H1; K, *Kpn*I; N, *Nsi*I; R, *Eco*RI; S, *Sac*I; E2-E4, exons 2–4. (*B–E*) ISH of a Raldh2 antisense riboprobe (*B* and *C*) and immunohistochemistry with an anti-RALDH2 polyclonal antibody (*D* and *E*) show an overall decrease of Raldh2 transcript and protein levels in E9.5 Raldh2$^{neo/-}$ embryos (*C* and *E*) when compared with Raldh2$^{+/-}$ control embryos (*B* and *D*). Region-specific differences of expression levels seem, however, to be preserved in mutants. (*B* and *C Insets*) Embryos hybridized with an exon 4-specific riboprobe. (*D* and *E Insets*) correspond to enlarged views of the mid-trunk region. (*F* and *G*) 5-Bromo-4-chloro-3-indolyl β-D-galactoside staining of Raldh2$^{+/-}$ (*F*) and Raldh2$^{neo/-}$ (*G*) embryos carrying a RARE-hsp68-lacZ reporter transgene (16) show a markedly decreased activity of the RA-responsive transgene in the mutant. ISH of a lacZ antisense riboprobe confirms the down-regulation of transgene activity in the Raldh2$^{neo/-}$ embryos (see *Insets*, which show comparative views of the mid-trunk region).

Results

The Raldh2^{neo} allele, which was originally generated in ES cells to allow Cre-mediated conditional mutagenesis, contains a floxed (f flanked with *lox*P sites) *PGK-neo* selectable marker in the fourth intron and a single *loxP* site in the third intron (Fig. 1*A*). Because several previously engineered alleles with intronic *PGK-neo* insertions have been found to behave as hypomorphs (e.g., ref. 17), we generated mutant mice that were either homozygous for the *Raldh2^{neo}* allele or carried one *Raldh2^{neo}* and one null allele (*Raldh2$^{neo/-}$*). No living *Raldh2$^{neo/-}$* mice could be identified at ≈postnatal (P) day 14 in the progeny of *Raldh2$^{+/neo}$* × *Raldh2$^{\pm}$* crosses, whereas 13 *Raldh2$^{neo/neo}$* mutants were identified in litters (187 pups) from *Raldh2$^{+/neo}$* intercrosses. Thus, ≈75% of the *Raldh2$^{neo/neo}$* mutants, and all *Raldh2$^{neo/-}$* compound mutants, died before the age of 2 weeks. Litters from the same intercrosses were collected at various developmental stages. Both the *Raldh2$^{neo/-}$* and *Raldh2$^{neo/neo}$* mutants were obtained at Mendelian ratios at embryonic (E9.5–12.5) and fetal (E13.5–14.5) stages. Sampling of E18.5 and newborn (P1) litters for phenotypic analysis confirmed that the death of both the *Raldh2$^{neo/-}$* and *Raldh2$^{neo/neo}$* mutants occurred during early postnatal life (see below).

The effect of the *Raldh2^{neo}* mutation on RALDH2 transcript and protein levels was analyzed by whole-mount ISH and immunochemistry, respectively. Using a full-length probe, E9.5 *Raldh2$^{neo/-}$* embryos exhibited an overall decrease of Raldh2 transcripts, even though their tissue distribution was similar to that of control (*Raldh2$^{+/-}$*) littermates (Fig. 1 *B* and *C*). A similar result was obtained with a fourth exon-specific probe (located upstream of the neo insertion), demonstrating that the decreased ISH signals do not result from lack of transcribed sequences located downstream of the neo insertion (Fig. 1 *B* and *C Insets*). Immunochemistry analysis using a RALDH2 polyclonal antibody revealed a similar decrease of protein levels in *Raldh2$^{neo/-}$* mutants (Fig. 1 *D* and *E*).

To investigate the effect of the *Raldh2^{neo}* mutation on embryonic RA levels, *Raldh2^{neo}* mice were crossed with an RA-reporter transgenic line (16). The pattern of RARE-*lacZ* reporter activity was spatially similar to that of *Raldh2* transcripts in E9.5 control embryos (compare Fig. 1 *B* and *F*). Whole-mount 5-bromo-4-chloro-3-indolyl β-D-galactoside assays revealed a marked overall decrease of RA-reporter transgene activity in *Raldh2$^{neo/-}$* embryos (Fig. 1*G*), which was confirmed by whole-mount ISH analysis of *lacZ* transcripts (Fig. 1 *F* and *G Insets*) and by quantitation of β-galactosidase activity in embryo protein extracts (data not shown).

Raldh2$^{neo/-}$ and *Raldh2$^{neo/neo}$* phenotypic defects were investigated by dissection of animals collected by Cesarean section at E18.5 or as newborns at P1, whole skeletal staining at E18.5-P1, and histological analysis at E14.5 and E18.5-P1. Most of the mutants recovered at E18.5 or P1 were alive, but they developed signs of cyanosis and suffocation within a few hours. Except for a slightly smaller size, the mutants showed no visible external defect. Lack of septation of the heart outflow tract into aorta and pulmonary trunk (persistent truncus arteriosus, PTA) was seen macroscopically or histologically in all *Raldh2$^{neo/-}$* mutants (Fig. 2*B* and data not shown). A ventricular septal defect was consistently associated (data not shown), as seen in human cases of PTA (18). No other heart defect was otherwise seen histologically (data not shown). The severity of the outflow tract septation defect appeared to depend on *Raldh2* gene dosage, as five of seven *Raldh2$^{neo/-}$* mutants exhibited a complete PTA (Fig. 2*B* and data not shown), whereas the two others displayed poorly developed conotruncal wedges (data not shown), and three of four *Raldh2$^{neo/neo}$* mutants displayed signs of partial septation (Fig. 2*C* and data not shown).

All *Raldh2$^{neo/-}$* and *Raldh2$^{neo/neo}$* mutants examined at E18.5 or P1 (n = 12) exhibited abnormal patterns of the aortic arch and/or head and neck great arteries. Two *Raldh2$^{neo/-}$* animals (Fig. 2 *F* and *G*) had a right-sided aortic arch, one with a double arch (Fig. 2*G*). The right subclavian artery (RSA) originated ectopically from the descending aorta, and the left subclavian artery (LSA) and left carotid arteries arose from a common trunk or innominate artery (Fig. 2 *F* and *G*). In WT, the innominate artery gives rise to the RSA and right common carotid artery (Fig. 2 *D* and *E*). Mutants with a left-sided aortic arch also displayed abnormal patterns of subclavian and carotid arteries (Fig. 2 *H* and *I*). The innominate artery was often absent, such that the RSA originated directly from the ascending aorta (Fig. 2*H*). Most *Raldh2$^{neo/-}$* and *Raldh2$^{neo/neo}$* mutants lacked, or exhibited shorter, common carotid arteries (right and left common carotid), their internal and external carotids arising from

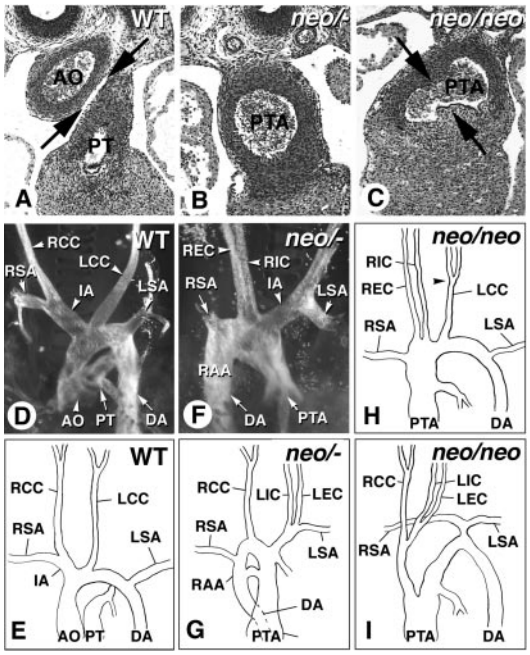

Fig. 2. Outflow tract septation defects and abnormal patterns of aortic arch-derived arteries in Raldh2^{neo} mutants. (*A–C*) Histological sections of the heart outflow tract region of E14.5 fetuses show fully separated aortic (AO) and pulmonary (PT) trunks in WT (*A*, arrows), whereas Raldh2$^{neo/-}$ (*B*) and Raldh2$^{neo/neo}$ (*C*) mutants exhibit an unseptated (PTA) or partially septated (arrows) outflow tract. Hematoxylin-eosin staining. (*D* and *E*) WT anatomy of the large arterial vessels, as observed after visualization of the arterial walls after alizarin red-alcian blue staining (*D*) or drawn from macroscopic examination (*E*) of newborn mice. (*F* and *G*) Arterial patterns of two Raldh2$^{neo/-}$ mutants (*F*, alizarin red-alcian blue staining; *G*, drawing from a newborn specimen). Both mutants show a right-sided aortic arch (RAA), such that the innominate artery (IA) gives rise to the LSA and carotid arteries, instead of the RSA and right common carotid (RCC). The descending aorta (DA) eventually reaches a normal left-sided thoracic position. Premature separation of the external and internal carotid arteries (REC and RIC in *F*; LEC and LIC in *G*) is also seen. (*H* and *I*) Arterial patterns of two Raldh2$^{neo/neo}$ newborn mutants. The animal in *H* lacked an innominate artery and its RSA, whereas its right internal (RIC) and external (REC) carotid arteries originated independently along the ascending aorta, and its left internal and external carotids (LIC and LEC) arose prematurely from the common carotid (LCC) at mid-cervical level (arrowhead). The mutant in *I* showed an abnormally high (cervical) aortic arch and ectopic origins of the left carotid arteries (LIC and LEC) and RSA.

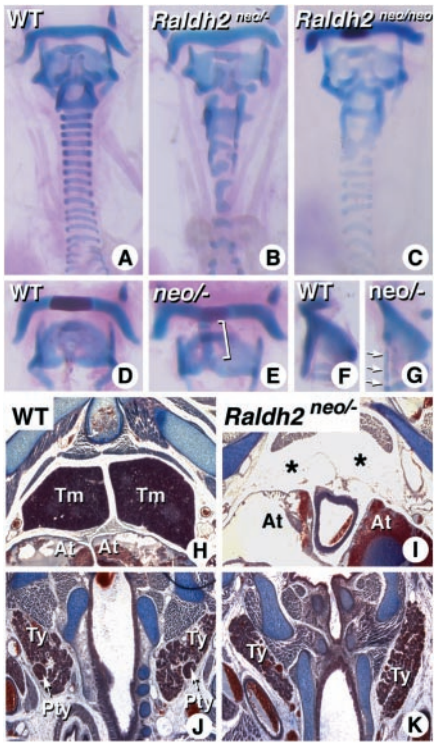

Fig. 3. Abnormal development of the laryngeal and tracheal cartilages, thymus, and parathyroid glands in Raldh2^{neo} mutant mice. (*A–C*) Comparison of the laryngeal and tracheal cartilages of E18.5 WT (*A*), Raldh2$^{neo/-}$ (*B*), and Raldh2$^{neo/neo}$ (*C*) mice. Alizarin red-alcian blue staining. (*D* and *E*) Hyoid and thyroid cartilages of WT and Raldh2$^{neo/-}$ mice, respectively. An ectopic cartilage connects these two elements in the mutant (bracket). (*F* and *G*) Profile views of the cricoid cartilage and first tracheal ring of WT and Raldh2$^{neo/-}$ mice, respectively. The posterior aspect of this cartilage is abnormally segmented in the mutant (arrows). (*H* and *I*) Coronal sections through the upper mediastinum of WT and Raldh2$^{neo/-}$ newborn mice, respectively, showing the absence of thymus (Tm) in the mutant (asterisks). At, atria. (*J* and *K*) Sections through the lateral portions of the thyroid gland (Ty) of WT and Raldh2$^{neo/-}$ newborn mice, respectively, showing a lack of parathyroid glands (Pty) in the mutant; tetrachrome staining.

the aortic arch (REC and RIC in Fig. 2 *F* and *H*), the innominate artery (LEC and LIC in Fig. 2*G*), or at midtracheal (instead of upper cervical) level (REC and RIC in Fig. 2*F*; LEC and LIC in Fig. 2*G*). One *Raldh2*$^{neo/neo}$ mutant exhibited an abnormally high (cervical) aortic arch and an abnormal origin of the RSA, which arose distally as a common stem with the LSA, whereas its carotid arteries arose from a common proximal innominate artery (Fig. 2*H*). An ectopic origin of the LSA from the ductus arteriosus was also observed in one *Raldh2*$^{neo/neo}$ mutant (data not shown). These defects are likely to result from an abnormal development or remodeling of the embryonic aortic arch system (see below).

Abnormalities of the heart outflow tract and large vessels are the major defects of the human DGS (13). Other characteristic features of this syndrome are the presence of a shorter trachea, with reduced number of tracheal rings, that may result from deficient blood supply in the fetal cervical region (19), as well as hypoplasia or aplasia of the thymus and parathyroid glands (12). A short trachea, with highly abnormal tracheal rings, was characteristic of *Raldh2*$^{neo/-}$ mutants (Fig. 3*B*). As seen for the outflow tract septation defects, *Raldh2*$^{neo/neo}$ mice displayed a milder version of this phenotype, with slightly reduced cartilage ring numbers (Fig. 3*C*). Abnormalities of the laryngeal cartilages were also detected in *Raldh2*$^{neo/-}$ mutants (Fig. 3 *D–G*, note the abnormal cartilaginous link between the hyoid bone and the thyroid cartilage and the abnormal segmentation of the cricoid cartilage into ring-like structures in *E* and *G*, respectively). The body of the hyoid bone and the laryngeal cartilages develop from the mesenchyme of the third and fourth to sixth branchial arches, respectively (18). No abnormality of more rostrally derived skeletal structures was seen in *Raldh2*^{neo} mutants (data not shown). Most of the mutants (9 of 10) displayed aplasia or marked hypoplasia of the thymus (Fig. 3 *H* and *I*). The WT parathyroid glands are embedded within the lateral regions of the thyroid gland (Fig. 3*J*). Whereas the thyroid gland was well formed in *Raldh2*^{neo} mutants, no parathyroid glands were found at the expected location (Fig. 3*K*).

DGS is thought to involve an embryonic defect restricted to the posterior most (third or fourth to sixth) branchial arches and the corresponding pharyngeal pouches (13, 20). We therefore investigated the embryonic basis of the *Raldh2*^{neo} phenotype. At E9.5, *Raldh2*$^{neo/-}$ mutants could be identified by their apparent lack of third branchial arches (e.g., Fig. 4*J*). Histological analysis showed well developed first and second arches, whereas the putative third to sixth arch region was very poorly developed

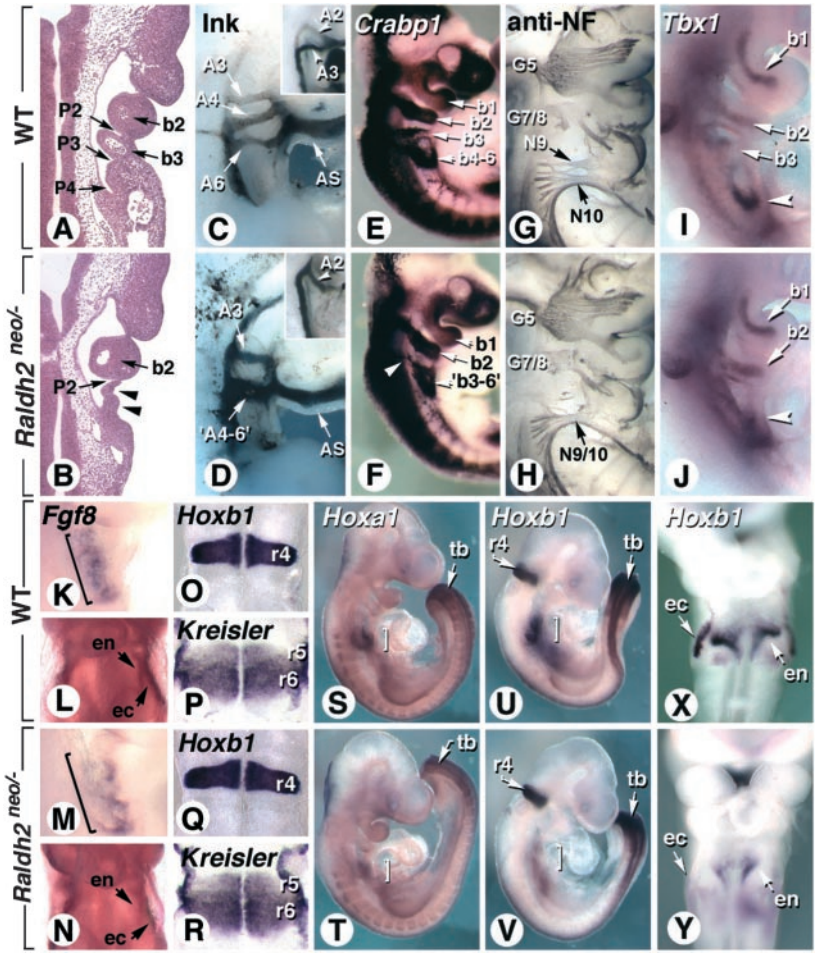

Fig. 4. Regionally restricted phenotypic defects and altered gene expression patterns in the posterior pharyngeal region of Raldh2$^{neo/-}$ embryos. (*A* and *B*) Coronal sections through the branchial arch region of E9.5 WT (*A*) and Raldh2$^{neo/-}$ (*B*) embryos (hematoxylin-eosin staining) show a marked hypoplasia of the putative third and fourth to sixth arches in the mutant, despite the presence of recognizable ectodermal clefts (arrowheads). b2 and b3, branchial arches; P2–P4, pharyngeal pouches. (*C* and *D*) Intracardial China ink injection allows to visualize the third, fourth, and sixth aortic arches (A3–A6) in E11.5 WT embryos (*C*). In Raldh2$^{neo/-}$ embryos, the arterial flow passes through the third aortic arches (A3) and a single enlarged posterior arch ('A4–6'). AS, aortic sac. Injections performed at an earlier stage (E9.5, *Insets*) show delayed development of the third aortic arches in mutants. (*E* and *F*) ISH of E9.5 embryos with a Crabp1 probe, a marker for migratory NCC, shows abnormal NCC patterning caudally to the second branchial arch (b2) in the mutant embryo (*F*). Instead of forming separate streams colonizing the third (b3) and fourth to sixth (b4–6) arches, cells are arranged in a single mass ('b3–6'), which is poorly connected with the hindbrain (arrowhead). (*G* and *H*) Antineurofilament immunostaining of E11.5 embryos reveals an abnormal fusion of the developing 9th and 10th cranial nerves (N9/10) in the mutant (*H*). G5 and G7/8, trigeminal and facial-acoustic ganglia, respectively. (*I* and *J*) ISH of E9.5 embryos with a Tbx1 probe shows reduced expression in the mutant posterior pharyngeal endoderm (*J*, arrowhead). (*K–N*) Hybridization of a Fgf8 probe (E9.5) shows weak and heterogeneous expression in the mutant posterior pharyngeal ectoderm (brackets), and almost undetectable expression in the underlying endoderm (compare *L* and *N*). (*O–R*) ISH with Hoxb1 (E9.5, *O* and *Q*) and kreisler (E8.5, *P* and *R*) probes, which mark rhombomeres (r) 4 and r5-r6, respectively, show comparable patterns in WT (*K* and *L*) and mutants (*M* and *N*). Hindbrains are viewed as flat-mount preparations. (*S* and *T*) Hybridization of a Hoxa1 probe (E9.5) shows abnormally low expression levels in the mutant pharyngeal region (brackets), whereas expression in the tail bud region (tb) seems unaffected. (*U* and *V*) Similarly, Hoxb1 expression is markedly decreased in the pharyngeal area of mutant embryos (brackets), whereas its expression in rhombomere 4 (r4) and in caudal tissues (tb) is comparable to that seen in WT. (*X* and *Y*) Frontal examination of the branchial arch region shows that down-regulation of Hoxb1 expression occurs in both the ectodermal (ec) and endodermal (en) layers.

(Fig. 4 *A* and *B*). The second pharyngeal pouch was properly formed. However, whereas more posterior ectodermal clefts were identified, there was no sign of distinct third or fourth pharyngeal pouches (Fig. 4*B*). Intracardial ink injections were performed at various developmental stages to visualize the embryonic aortic arch system. At E9.5, such injections labeled the second and third aortic arches in WT embryos (Fig. 4*C Inset*). However, no third aortic arches were formed in *Raldh2*$^{neo/-}$ embryos (Fig. 4*D Inset*). The third aortic arches became apparent at E10.5 in mutant embryos (data not shown). Whereas distinct fourth and sixth aortic arches were formed at E11.5 in WT (Fig. 4*C*), the mutant embryos exhibited a single, enlarged vessel caudal to their third arches (Fig. 4*D*, A4–6′).

Neural crest cells (NCC) originating from the posterior hindbrain and migrating through the third, fourth, and sixth branchial arches give rise to a cardiac NCC population, which is required for proper septation of the outflow tract (21). *Crabp1* mRNA was used as a molecular marker of migrating NCC in E9.5 WT (Fig. 4*E*) and *Raldh2*$^{neo/-}$ (Fig. 4*F*) embryos. A substantial NCC population was present in the posterior branchial region of mutant embryos (Fig. 4*F*). However, these cells were not organized in distinct segmental migratory pathways as in WT embryos (Fig. 4*E*). In contrast, the migratory pathways of more rostral NCC populations (e.g., toward branchial arches 1 and 2) were unaltered in mutant embryos. Analysis of *AP2α* (22) transcripts and the *Wnt1-lacZ* transgene (23) at E9.0 also

indicated that there was no deficiency in pre- or early migratory NCC in *Raldh2*$^{neo/-}$ mutants (data not shown). Furthermore, a *Kreisler*-labeled migratory cell population was present in E8.5 *Raldh2*$^{neo/-}$ embryos (data not shown). Interestingly, *Kreisler* transcripts specifically mark rhombomere 6-derived NCC, which migrate into the third branchial arches in WT embryos.

We also analyzed cranial nerve development in mutant embryos. Antineurofilament staining at E9.5 revealed a normal patterning of the Vth (trigeminal) and VIIth–VIIIth (facial-acoustic) cranial nerve ganglia and distal branches, which innervate first and second branchial arch derivatives, respectively (Fig. 4*H*). However, the fibers that should contribute to cranial nerves IX (glosso-pharyngeal) and X (vagus) merged in a single bundle and failed to form separate distal ganglia (compare Fig. 4 *G* and *H*). Using *c-ret* as a molecular marker of the facial-acoustic ganglion complex at E10.5, we found very few positive cells posteriorly to the otocyst, at the expected level of the glossopharyngeal and vagal ganglia (data not shown). In addition, *Neurogenin2* (*ngn2*) transcript analysis revealed an abnormal fusion of the second and third epibranchial placodes in E9.5 *Raldh2*$^{neo/-}$ embryos (data not shown). Hence, as seen for migratory NCC, cranial nerve developmental defects are restricted to the postotic branchial region in *Raldh2*$^{neo/-}$ mutants.

The *Raldh2*^{neo} aortic arch phenotype (Fig. 4*D*) is reminiscent of that of *Tbx1*$^{-/-}$ knockout embryos (24–26). We therefore investigated whether *Tbx1* expression may be altered in *Raldh2*$^{neo/-}$ embryos. *Tbx1* expression was unaffected in the core mesenchyme of the first and second mutant branchial arches (compare Fig. 4 *I* and *J*). *Tbx1* mesenchymal expression was detected in the mutant posterior branchial region, which may correspond to the third arch core mesenchymal expression seen in WT embryos (Fig. 4*J*, arrow). *Tbx1* was also expressed in the mutant posterior pharyngeal endoderm, although its expression seemed somewhat reduced and not as sharply defined as in WT littermates (compare Fig. 4 *I* and *J*). Whether this alteration may be a cause or a consequence of the lack of development of third and fourth pharyngeal pouches is unknown. Hypomorphic mutations of the mouse *Fgf8* gene lead to posterior branchial arch defects (27, 28) similar to those seen in mouse models for DGS (24–26), and *Fgf8* expression is selectively altered in the posterior branchial region of *Tbx1*$^{-/-}$ mouse mutants (29). We analyzed *Fgf8* expression in E9.5 *Raldh2*$^{neo/-}$ embryos and found that its expression was abnormally low and/or patchy in both the ectoderm and endoderm of the posterior pharyngeal region (compare Fig. 4 *K* and *L* with *M* and *N*).

We have previously reported that *Raldh*$^{-/-}$ null mutants exhibit severe growth and patterning defects of the posterior hindbrain region (11). Several rhombomeric markers were therefore analyzed in *Raldh2*$^{neo/-}$ embryos. The hindbrain expression patterns of *Hoxb1* (Fig. 4 *O* and *Q*), *kreisler* (Fig. 4 *P* and *R*), and *Hoxd4* (data not shown), which mark, respectively, rhombomeres 4, 5/6, and 7, were not detectably altered in the *Raldh2*$^{neo/-}$ mutants, thus excluding a primary defect of hindbrain growth or patterning.

The *Hoxa1* and *Hoxb1* homeobox genes are two *in vivo* RA target genes (30). When analyzed in *Raldh2*$^{neo/-}$ embryos, expression of both genes seemed to be selectively down-regulated in the posterior branchial arch and foregut region (Fig. 4 *S–V*). Expression of both genes in the tail bud region, as well as *Hoxb1* expression in rhombomere 4, was similar in WT and mutant embryos (Fig. 4 *S–V*, see also *X* and *Y*). Expression of both genes was altered in both the endodermal and ectodermal layers of the pharyngeal region (Fig. 4 *X* and *Y* and data not shown). Expression of *Rarβ*, another direct RA-target gene, was also selectively affected in the posterior pharyngeal endoderm and mesoderm, whereas its expression in more rostral pharyngeal areas or in the neural tube was not altered in *Raldh2*$^{neo/-}$ mutants (data not shown).

Discussion

Although the *Raldh2* hypomorphic mutation leads to an overall decrease of its mRNA and protein gene products, as well as of the activity of an RA-responsive reporter transgene in the embryo, its phenotypic consequences are strikingly restricted to a subset of tissues whose development requires RA (9, 11). Most interestingly, the observed defects, which also correspond to a subset of the spectrum of congenital abnormalities resulting from dietary vitamin A deficiency in rats (5) or compound RAR gene knockouts in mice (31), recapitulate the traits of the DGS, a relatively frequent (1:5,000–1:10,000 live births) human disorder characterized by heart outflow tract septation defects, abnormal patterning of the aortic arch derivatives, and hypoplasia or aplasia of the thymus and parathyroid glands (12, 13). This syndrome is thought to result from developmental defect(s) arising in the region of the third and fourth branchial arches and the corresponding pharyngeal pouches. Our analysis of *Raldh2*$^{neo/-}$ embryos revealed specific defects of the third to sixth branchial arch region. The observed defects are consistent with those that have been described in cultured mouse embryos that were treated with a synthetic RAR antagonist at early stages of branchial arch formation (32). Taken all together, our results indicate that cardiac NCC, which do not seem to be initially deficient in *Raldh2*^{neo} embryos, are perturbed in their migratory pathways and/or developmental potential due to severe morphological and molecular defects of the posterior pharyngeal endoderm. We conclude that RA normally synthesized by RALDH2 in the posterior pharyngeal mesoderm (unpublished data) is an important signal to correctly pattern the adjacent endoderm and the cardiac NCC.

In humans, the DGS abnormalities are often associated with additional craniofacial defects such as telecanthus (short palpebral fissures), micrognathia, small and low set ears, and/or cleft palate. This association, known as velocardiofacial (VCFS) or Shprintzen syndrome (33, 34), most often (≈90%) results from heterozygous microdeletions on the long arm of chromosome 22 (22q11.2del) (35–37). Several groups have recently engineered chromosomal deletions in the murine region homologous to the 22q11.2 human region (38–40). Their work led to the conclusion that several genes may be involved in the pathogenesis of the 22q11.2del DGS/VCFS abnormalities, among which *Tbx1* (24, 25, 40) and *Crko1* (41) may be two critical determinants. Whereas heterozygous disruption of mouse *Tbx1* generates specific defects of the fourth aortic arches (24) and their derivatives (40), homozygous disruption of these two genes leads to defects along the entire branchial arch region, as well as (in the case of *Tbx1*) in more anterior skull structures (24, 25). However, *Raldh2*$^{neo/-}$ mutants did not exhibit any strong alteration of *Tbx1* expression, as well as of other genes expressed in the developing arch mesenchyme and endoderm (e.g., *HRT1* and *dH* and, data not shown). Thus, the *Raldh2*$^{neo/-}$ DGS-like syndrome is likely to result from pharyngeal molecular alterations that may be independent (e.g., *Hoxa1* and *Hoxb1* deficiency, ref. 42) or occur downstream (as suggested for *Fgf8*, ref. 29) of *Tbx1* function.

Despite the frequent occurrence of 22q11.2 deletions in patients with DGS/VCFS features, DGS has long been recognized as an etiologically heterogeneous syndrome (37), which may involve other genetic loci (such as 10p3) (43, 44), as well as epigenetic and/or environmental causes. Our data, which demonstrate that caudal branchial arches are exquisitely sensitive to RA deficiency, indicate that decreased levels of embryonic RA could be one of these causes. Even rather subtle impairments of RA synthetic ability (e.g., through heterozygous mutation of *RALDH2*) could be potentiated by situations of vitamin A deficiency, resulting from insufficient or imbalanced nutritional intake (e.g., in the case of anorexia). Whereas severe vitamin A

deficiency is unlikely to be seen in developed countries, an important risk factor could be embryonic exposure to ethanol, as it may act as a competitive inhibitor of alcohol dehydrogenase(s) that act upstream of RALDH enzymes to catalyze the first step in the conversion of retinol to RA (45). It is noteworthy that DGS abnormalities have been described in children with clinical evidence of fetal alcohol syndrome (46). More generally, our study demonstrates that alterations of RA signaling should also be considered as possible modifiers of the DGS/VCFS phenotypes, including in the case of 22q11 deletion-linked syndromes whose expressivity is highly variable, even within a single family or among monozygotic twins (47).

We thank B. Schuhbaur and Olivier Gardon for excellent technical assistance; M. Le Meur and S. Falcone for animal care; J. Rossant (Mount Sinai Hospital Research Institute, Toronto) for providing the RARE-hsp68-lacZ transgenic mice; P. McCaffery and U. Dräger (Eunice Kennedy Shriver Center, Waltham, MA) for the RALDH2 antibody; and R. Loury and J. Sutter for sharing discussion. This work was supported by funds from the Centre National de la Recherche Scientifique, the Institut National de la Santé et de la Recherche Médicale, the Collège de France, the Hôpitaux Universitaires de Strasbourg, the Association pour la Recherche sur le Cancer, and the Fondation pour la Recherche Médicale. J.V. was supported by fellowships from the Ministère de la Recherche and the Association pour la Recherche sur le Cancer.

1. Mangelsdorf, D. J. (1994) *Nutr. Rev.* **52,** S32–S44.
2. Chambon, P. (1996) *FASEB J.* **10,** 940–954.
3. Mollard, R., Viville, S., Ward, S. J., Decimo, D., Chambon, P. & Dolle, P. (2000) *Mech. Dev.* **94,** 223–232.
4. Kastner, P., Mark, M. & Chambon, P. (1995) *Cell* **83,** 859–869.
5. Wilson, J. G., Roth, C. B. & Warkany, J. (1953) *Am. J. Anat.* **92,** 189–217.
6. Zhao, D., McCaffery, P., Ivins, K. J., Neve, R. L., Hogan, P., Chin, W. W. & Drager, U. C. (1996) *Eur. J. Biochem.* **240,** 15–22.
7. Mic, F. A., Molotkov, A., Fan, X., Cuenca, A. E. & Duester, G. (2000) *Mech. Dev.* **97,** 227–230.
8. Niederreither, K., McCaffery, P., Drager, U. C., Chambon, P. & Dolle, P. (1997) *Mech. Dev.* **62,** 67–78.
9. Niederreither, K., Subbarayan, V., Dolle, P. & Chambon, P. (1999) *Nat. Genet.* **21,** 444–448.
10. Niederreither, K., Vermot, J., Messaddeq, N., Schuhbaur, B., Chambon, P. & Dolle, P. (2001) *Development (Cambridge, U.K.)* **128,** 1019–1031.
11. Niederreither, K., Vermot, J., Schuhbaur, B., Chambon, P. & Dolle, P. (2000) *Development (Cambridge, U.K.)* **127,** 75–85.
12. DiGeorge, A. M. (1968) *Birth Defects Orig. Art. Ser.* **4,** 116–121.
13. Conley, M. E., Beckwith, J. B., Mancer, J. F. & Tenckhoff, L. (1979) *J. Pediatr.* **94,** 883–890.
14. Mark, M., Lufkin, T., Vonesch, J. L., Ruberte, E., Olivo, J. C., Dolle, P., Gorry, P., Lumsden, A. & Chambon, P. (1993) *Development (Cambridge, U.K.)* **119,** 319–338.
15. Décimo, D., Georges-Labouesse, E. & Dollé, P. (1995) in *Gene Probes 2: A Practical Approach*, eds. Hames, B. D. & Higgins, S. J. (Oxford Univ. Press, New York), pp. 183–210.
16. Rossant, J., Zirngibl, R., Cado, D., Shago, M. & Giguere, V. (1991) *Genes Dev.* **5,** 1333–1344.
17. Meyers, E. N., Lewandoski, M. & Martin, G. R. (1998) *Nat. Genet.* **18,** 136–141.
18. Larsen, W. J. (1993) *Human Embryology* (Churchill Livingstone, New York).
19. Sein, K., Wells, T. R., Landing, B. H. & Chow, C. R. (1985) *Pediatr. Pathol.* **4,** 81–88.
20. Freedom, R. M., Rosen, F. S. & Nadas, A. S. (1972) *Circulation* **46,** 165–172.
21. Waldo, K. L., Kumiski, D. & Kirby, M. L. (1996) *Dev. Dyn.* **205,** 281–292.
22. Mitchell, P. J., Timmons, P. M., Hebert, J. M., Rigby, P. W. & Tjian, R. (1991) *Genes Dev.* **5,** 105–119.
23. Echelard, Y., Vassileva, G. & McMahon, A. P. (1994) *Development (Cambridge, U.K.)* **120,** 2213–2224.
24. Lindsay, E. A., Vitelli, F., Su, H., Morishima, M., Huynh, T., Pramparo, T., Jurecic, V., Ogunrinu, G., Sutherland, H. F., Scambler, P. J., *et al.* (2001) *Nature* **410,** 97–101.
25. Jerome, L. A. & Papaioannou, V. E. (2001) *Nat. Genet.* **27,** 286–291.
26. Vitelli, F., Morishima, M., Taddei, I., Lindsay, E. A. & Baldini, A. (2002) *Hum. Mol. Genet.* **11,** 915–922.
27. Abu-Issa, R., Smyth, G., Smoak, I., Yamamura, K. & Meyers, E. N. (2002) *Development (Cambridge, U.K.)* **129,** 4613–4625.
28. Frank, D. U., Fotheringham, L. K., Brewer, J. A., Muglia, L. J., Tristani-Firouzi, M., Capecchi, M. R. & Moon, A. M. (2002) *Development (Cambridge, U.K.)* **129,** 4591–4603.
29. Vitelli, F., Taddei, I., Morishima, M., Meyers, E. N., Lindsay, E. A. & Baldini, A. (2002) *Development (Cambridge, U.K.)* **129,** 4605–4611.
30. Gavalas, A., Studer, M., Lumsden, A., Rijli, F. M., Krumlauf, R. & Chambon, P. (1998) *Development (Cambridge, U.K.)* **125,** 1123–1136.
31. Mendelsohn, C., Lohnes, D., Decimo, D., Lufkin, T., LeMeur, M., Chambon, P. & Mark, M. (1994) *Development (Cambridge, U.K.)* **120,** 2749–2771.
32. Wendling, O., Dennefeld, C., Chambon, P. & Mark, M. (2000) *Development (Cambridge, U.K.)* **127,** 1553–1562.
33. Goldberg, R., Motzkin, B., Marion, R., Scambler, P. J. & Shprintzen, R. J. (1993) *Am. J. Med. Genet.* **45,** 313–319.
34. Stevens, C. A., Carey, J. C. & Shigeoka, A. O. (1990) *Pediatrics* **85,** 526–530.
35. Driscoll, D. A., Budarf, M. L. & Emanuel, B. S. (1992) *Am. J. Hum. Genet.* **50,** 924–933.
36. Wilson, D. I., Burn, J., Scambler, P. & Goodship, J. (1993) *J. Med. Genet.* **30,** 852–856.
37. Shprintzen, R. J. (1994) *J. Med. Genet.* **31,** 423–424.
38. Lindsay, E. A., Botta, A., Jurecic, V., Carattini-Rivera, S., Cheah, Y. C., Rosenblatt, H. M., Bradley, A. & Baldini, A. (1999) *Nature* **401,** 379–383.
39. Puech, A., Saint-Jore, B., Merscher, S., Russell, R. G., Cherif, D., Sirotkin, H., Xu, H., Factor, S., Kucherlapati, R. & Skoultchi, A. I. (2000) *Proc. Natl. Acad. Sci. USA* **97,** 10090–10095.
40. Merscher, S., Funke, B., Epstein, J. A., Heyer, J., Puech, A., Lu, M. M., Xavier, R. J., Demay, M. B., Russell, R. G., Factor, S., *et al.* (2001) *Cell* **104,** 619–629.
41. Guris, D. L., Fantes, J., Tara, D., Druker, B. J. & Imamoto, A. (2001) *Nat. Genet.* **27,** 293–298.
42. Rossel, M. & Capecchi, M. R. (1999) *Development (Cambridge, U.K.)* **126,** 5027–5040.
43. Gottlieb, S., Driscoll, D. A., Punnett, H. H., Sellinger, B., Emanuel, B. S. & Budarf, M. L. (1998) *Am. J. Hum. Genet.* **62,** 495–498.
44. Monaco, G., Pignata, C., Rossi, E., Mascellaro, O., Cocozza, S. & Ciccimarra, F. (1991) *Am. J. Med. Genet.* **39,** 215–216.
45. Deltour, L., Ang, H. L. & Duester, G. (1996) *FASEB J.* **10,** 1050–1057.
46. Ammann, A. J., Wara, D. W., Cowan, M. J., Barrett, D. J. & Stiehm, E. R. (1982) *Am. J. Dis. Child.* **136,** 906–908.
47. Vincent, M.-C., Heitz, F., Tricoire, J., Bourrouillou, G., Kuhlein, E., Rolland, M. & Calvas, P. (1999) *Genet. Counsel.* **10,** 43–49.